Nuclear Dependence of the Transverse-Single-Spin Asymmetry for Forward Neutron Production in Polarized p+A Collisions at √sNN=200 GeV

(PHENIX Collaboration) Aidala, C.; ...; Dumancic, Mirta; ...; Makek, Mihael; ...; Vukman, Nikola; ...; Zou, L.

Nuclear Dependence of the Transverse-Single-Spin Asymmetry for Forward Neutron Production in Polarized $p+A$ Collisions at $\sqrt{s_{NN}} = 200$ GeV

C. Aidala,[40] Y. Akiba,[51,52,†] M. Alfred,[22] V. Andrieux,[40] K. Aoki,[30] N. Apadula,[27] H. Asano,[33,51] C. Ayuso,[40] B. Azmoun,[7] V. Babintsev,[23] A. Bagoly,[16] N. S. Bandara,[39] K. N. Barish,[8] S. Bathe,[5,52] A. Bazilevsky,[7] M. Beaumier,[8] R. Belmont,[12] A. Berdnikov,[54] Y. Berdnikov,[54] D. S. Blau,[32,43] M. Boer,[35] J. S. Bok,[45] M. L. Brooks,[35] J. Bryslawskyj,[5,8] V. Bumazhnov,[23] C. Butler,[20] S. Campbell,[13] V. Canoa Roman,[57] R. Cervantes,[57] C. Y. Chi,[13] M. Chiu,[7] I. J. Choi,[24] J. B. Choi,[10,*] Z. Citron,[62] M. Connors,[20,52] N. Cronin,[57] M. Csanád,[16] T. Csörgő,[17,63] T. W. Danley,[46] M. S. Daugherity,[1] G. David,[7,57] K. DeBlasio,[44] K. Dehmelt,[57] A. Denisov,[23] A. Deshpande,[52,57] E. J. Desmond,[7] A. Dion,[57] D. Dixit,[57] J. H. Do,[64] A. Drees,[57] K. A. Drees,[6] M. Dumancic,[62] J. M. Durham,[35] A. Durum,[23] T. Elder,[20] A. Enokizono,[51,53] H. En'yo,[51] S. Esumi,[60] B. Fadem,[41] W. Fan,[57] N. Feege,[57] D. E. Fields,[44] M. Finger,[9] M. Finger, Jr.,[9] S. L. Fokin,[32] J. E. Frantz,[46] A. Franz,[7] A. D. Frawley,[19] Y. Fukuda,[60] C. Gal,[57] P. Gallus,[14] P. Garg,[3,57] H. Ge,[57] F. Giordano,[24] Y. Goto,[51,52] N. Grau,[2] S. V. Greene,[61] M. Grosse Perdekamp,[24] T. Gunji,[11] H. Guragain,[20] T. Hachiya,[51,52] J. S. Haggerty,[7] K. I. Hahn,[18] H. Hamagaki,[11] H. F. Hamilton,[1] S. Y. Han,[18] J. Hanks,[57] S. Hasegawa,[28] T. O. S. Haseler,[20] X. He,[20] T. K. Hemmick,[57] J. C. Hill,[27] K. Hill,[12] R. S. Hollis,[8] K. Homma,[21] B. Hong,[31] T. Hoshino,[21] N. Hotvedt,[27] J. Huang,[7] S. Huang,[61] K. Imai,[28] J. Imrek,[15] M. Inaba,[60] A. Iordanova,[8] D. Isenhower,[1] Y. Ito,[42] D. Ivanishchev,[50] B. V. Jacak,[57] M. Jezghani,[20] Z. Ji,[57] X. Jiang,[35] B. M. Johnson,[7,20] V. Jorjadze,[57] D. Jouan,[48] D. S. Jumper,[24] J. H. Kang,[64] D. Kapukchyan,[8] S. Karthas,[57] D. Kawall,[39] A. V. Kazantsev,[32] V. Khachatryan,[57] A. Khanzadeev,[50] C. Kim,[8,31] D. J. Kim,[29] E.-J. Kim,[10] M. Kim,[55] M. H. Kim,[31] D. Kincses,[16] E. Kistenev,[7] J. Klatsky,[19] P. Kline,[57] T. Koblesky,[12] D. Kotov,[50,54] S. Kudo,[60] K. Kurita,[53] Y. Kwon,[64] J. G. Lajoie,[27] E. O. Lallow,[41] A. Lebedev,[27] S. Lee,[64] M. J. Leitch,[35] Y. H. Leung,[57] N. A. Lewis,[40] X. Li,[35] S. H. Lim,[35,64] L. D. Liu,[49] M. X. Liu,[35] V.-R. Loggins,[24] S. Lökös,[16,17] K. Lovasz,[15] D. Lynch,[7] T. Majoros,[15] Y. I. Makdisi,[6] M. Makek,[65] M. Malaev,[50] V. I. Manko,[32] E. Mannel,[7] H. Masuda,[53] M. McCumber,[35] P. L. McGaughey,[35] D. McGlinchey,[12,35] C. McKinney,[24] M. Mendoza,[8] W. J. Metzger,[17] A. C. Mignerey,[38] D. E. Mihalik,[57] A. Milov,[62] D. K. Mishra,[4] J. T. Mitchell,[7] G. Mitsuka,[52] S. Miyasaka,[51,59] S. Mizuno,[51,60] P. Montuenga,[24] T. Moon,[64] D. P. Morrison,[7] S. I. M. Morrow,[61] T. Murakami,[33,51] J. Murata,[51,53] K. Nagai,[59] K. Nagashima,[21] T. Nagashima,[53] J. L. Nagle,[12] M. I. Nagy,[16] I. Nakagawa,[51,52] H. Nakagomi,[51,60] K. Nakano,[51,59] C. Nattrass,[58] T. Niida,[60] R. Nouicer,[7,52] T. Novák,[17,63] N. Novitzky,[57] R. Novotny,[14] A. S. Nyanin,[32] E. O'Brien,[7] C. A. Ogilvie,[27] J. D. Orjuela Koop,[12] J. D. Osborn,[40] A. Oskarsson,[36] G. J. Ottino,[44] K. Ozawa,[30,60] V. Pantuev,[25] V. Papavassiliou,[45] J. S. Park,[55] S. Park,[51,55,57] S. F. Pate,[45] M. Patel,[27] W. Peng,[61] D. V. Perepelitsa,[7,12] G. D. N. Perera,[45] D. Yu. Peressounko,[32] C. E. PerezLara,[57] J. Perry,[27] R. Petti,[7] M. Phipps,[7,24] C. Pinkenburg,[7] R. P. Pisani,[7] A. Pun,[46] M. L. Purschke,[7] P. V. Radzevich,[54] K. F. Read,[47,58] D. Reynolds,[56] V. Riabov,[43,50] Y. Riabov,[50,54] D. Richford,[5] T. Rinn,[27] S. D. Rolnick,[8] M. Rosati,[27] Z. Rowan,[5] J. Runchey,[27] A. S. Safonov,[54] T. Sakaguchi,[7] H. Sako,[28] V. Samsonov,[43,50] M. Sarsour,[20] K. Sato,[60] S. Sato,[28] B. Schaefer,[61] B. K. Schmoll,[58] K. Sedgwick,[8] R. Seidl,[51,52] A. Sen,[27,58] R. Seto,[8] A. Sexton,[38] D. Sharma,[57] I. Shein,[23] T.-A. Shibata,[51,59] K. Shigaki,[21] M. Shimomura,[27,42] T. Shioya,[60] P. Shukla,[4] A. Sickles,[24] C. L. Silva,[35] D. Silvermyr,[36] B. K. Singh,[3] C. P. Singh,[3] V. Singh,[3] M. J. Skoby,[40] M. Slunečka,[9] K. L. Smith,[19] M. Snowball,[35] R. A. Soltz,[34] W. E. Sondheim,[35] S. P. Sorensen,[58] I. V. Sourikova,[7] P. W. Stankus,[47] S. P. Stoll,[7] T. Sugitate,[21] A. Sukhanov,[7] T. Sumita,[51] J. Sun,[57] S. Syed,[20] J. Sziklai,[63] A. Takeda,[42] K. Tanida,[28,52,55] M. J. Tannenbaum,[7] S. Tarafdar,[61,62] A. Taranenko,[43,56] G. Tarnai,[15] R. Tieulent,[20,37] A. Timilsina,[27] T. Todoroki,[60] M. Tomášek,[14] C. L. Towell,[1] R. S. Towell,[1] I. Tserruya,[62] Y. Ueda,[21] B. Ujvari,[15] H. W. van Hecke,[35] S. Vazquez-Carson,[12] J. Velkovska,[61] M. Virius,[14] V. Vrba,[14,26] N. Vukman,[65] X. R. Wang,[45,52] Z. Wang,[5] Y. Watanabe,[51,52] Y. S. Watanabe,[11] C. P. Wong,[20] C. L. Woody,[7] C. Xu,[45] Q. Xu,[61] L. Xue,[20] S. Yalcin,[57] Y. L. Yamaguchi,[52,57] H. Yamamoto,[60] A. Yanovich,[23] P. Yin,[12] J. H. Yoo,[31] I. Yoon,[55] H. Yu,[45,49] I. E. Yushmanov,[32] W. A. Zajc,[13] A. Zelenski,[6] S. Zharko,[54] and L. Zou[8]

(PHENIX Collaboration)

[1]*Abilene Christian University, Abilene, Texas 79699, USA*
[2]*Department of Physics, Augustana University, Sioux Falls, South Dakota 57197, USA*
[3]*Department of Physics, Banaras Hindu University, Varanasi 221005, India*
[4]*Bhabha Atomic Research Centre, Bombay 400 085, India*
[5]*Baruch College, City University of New York, New York, New York 10010, USA*

[6]Collider-Accelerator Department, Brookhaven National Laboratory, Upton, New York 11973-5000, USA
[7]Physics Department, Brookhaven National Laboratory, Upton, New York 11973-5000, USA
[8]University of California–Riverside, Riverside, California 92521, USA
[9]Charles University, Ovocný trh 5, Praha 1, 116 36, Prague, Czech Republic
[10]Chonbuk National University, Jeonju 561-756, Korea
[11]Center for Nuclear Study, Graduate School of Science, University of Tokyo,
7-3-1 Hongo, Bunkyo, Tokyo 113-0033, Japan
[12]University of Colorado, Boulder, Colorado 80309, USA
[13]Columbia University, New York, New York 10027, USA and Nevis Laboratories, Irvington, New York 10533, USA
[14]Czech Technical University, Zikova 4, 166 36 Prague 6, Czech Republic
[15]Debrecen University, H-4010 Debrecen, Egyetem tér 1, Hungary
[16]ELTE, Eötvös Loránd University, H-1117 Budapest, Pázmány P. s. 1/A, Hungary
[17]Eszterházy Károly University, Károly Róbert Campus, H-3200 Gyöngyös, Mátrai út 36, Hungary
[18]Ewha Womans University, Seoul 120-750, Korea
[19]Florida State University, Tallahassee, Florida 32306, USA
[20]Georgia State University, Atlanta, Georgia 30303, USA
[21]Hiroshima University, Kagamiyama, Higashi-Hiroshima 739-8526, Japan
[22]Department of Physics and Astronomy, Howard University, Washington, DC 20059, USA
[23]IHEP Protvino, State Research Center of Russian Federation, Institute for High Energy Physics, Protvino 142281, Russia
[24]University of Illinois at Urbana-Champaign, Urbana, Illinois 61801, USA
[25]Institute for Nuclear Research of the Russian Academy of Sciences, prospekt 60-letiya Oktyabrya 7a, Moscow 117312, Russia
[26]Institute of Physics, Academy of Sciences of the Czech Republic, Na Slovance 2, 182 21 Prague 8, Czech Republic
[27]Iowa State University, Ames, Iowa 50011, USA
[28]Advanced Science Research Center, Japan Atomic Energy Agency, 2-4 Shirakata Shirane,
Tokai-mura, Naka-gun, Ibaraki-ken 319-1195, Japan
[29]Helsinki Institute of Physics and University of Jyväskylä, P.O. Box 35, FI-40014 Jyväskylä, Finland
[30]KEK, High Energy Accelerator Research Organization, Tsukuba, Ibaraki 305-0801, Japan
[31]Korea University, Seoul 136-701, Korea
[32]National Research Center "Kurchatov Institute," Moscow 123098 Russia
[33]Kyoto University, Kyoto 606-8502, Japan
[34]Lawrence Livermore National Laboratory, Livermore, California 94550, USA
[35]Los Alamos National Laboratory, Los Alamos, New Mexico 87545, USA
[36]Department of Physics, Lund University, Box 118, SE-221 00 Lund, Sweden
[37]IPNL, CNRS/IN2P3, Univ Lyon, Universit Lyon 1, F-69622, Villeurbanne, France
[38]University of Maryland, College Park, Maryland 20742, USA
[39]Department of Physics, University of Massachusetts, Amherst, Massachusetts 01003-9337, USA
[40]Department of Physics, University of Michigan, Ann Arbor, Michigan 48109-1040, USA
[41]Muhlenberg College, Allentown, Pennsylvania 18104-5586, USA
[42]Nara Women's University, Kita-uoya Nishi-machi Nara 630-8506, Japan
[43]National Research Nuclear University, MEPhI, Moscow Engineering Physics Institute, Moscow 115409, Russia
[44]University of New Mexico, Albuquerque, New Mexico 87131, USA
[45]New Mexico State University, Las Cruces, New Mexico 88003, USA
[46]Department of Physics and Astronomy, Ohio University, Athens, Ohio 45701, USA
[47]Oak Ridge National Laboratory, Oak Ridge, Tennessee 37831, USA
[48]IPN-Orsay, Université Paris-Sud, CNRS/IN2P3, Université Paris-Saclay, BP1, F-91406 Orsay, France
[49]Peking University, Beijing 100871, People's Republic of China
[50]PNPI, Petersburg Nuclear Physics Institute, Gatchina, Leningrad region 188300, Russia
[51]RIKEN Nishina Center for Accelerator-Based Science, Wako, Saitama 351-0198, Japan
[52]RIKEN BNL Research Center, Brookhaven National Laboratory, Upton, New York 11973-5000, USA
[53]Physics Department, Rikkyo University, 3-34-1 Nishi-Ikebukuro, Toshima, Tokyo 171-8501, Japan
[54]Saint Petersburg State Polytechnic University, St. Petersburg 195251 Russia
[55]Department of Physics and Astronomy, Seoul National University, Seoul 151-742, Korea
[56]Chemistry Department, Stony Brook University, SUNY, Stony Brook, New York 11794-3400, USA
[57]Department of Physics and Astronomy, Stony Brook University, SUNY, Stony Brook, New York 11794-3800, USA
[58]University of Tennessee, Knoxville, Tennessee 37996, USA
[59]Department of Physics, Tokyo Institute of Technology, Oh-okayama, Meguro, Tokyo 152-8551, Japan
[60]Center for Integrated Research in Fundamental Science and Engineering,
University of Tsukuba, Tsukuba, Ibaraki 305, Japan
[61]Vanderbilt University, Nashville, Tennessee 37235, USA
[62]Weizmann Institute, Rehovot 76100, Israel

[63]Institute for Particle and Nuclear Physics, Wigner Research Centre for Physics, Hungarian Academy of Sciences (Wigner RCP, RMKI) H-1525 Budapest 114, P.O. Box 49, Budapest, Hungary
[64]Yonsei University, IPAP, Seoul 120-749, Korea
[65]Department of Physics, Faculty of Science, University of Zagreb, Bijenička c. 32 HR-10002 Zagreb, Croatia

(Received 3 April 2017; revised manuscript received 26 September 2017; published 8 January 2018)

During 2015, the Relativistic Heavy Ion Collider (RHIC) provided collisions of transversely polarized protons with Au and Al nuclei for the first time, enabling the exploration of transverse-single-spin asymmetries with heavy nuclei. Large single-spin asymmetries in very forward neutron production have been previously observed in transversely polarized $p+p$ collisions at RHIC, and the existing theoretical framework that was successful in describing the single-spin asymmetry in $p+p$ collisions predicts only a moderate atomic-mass-number (A) dependence. In contrast, the asymmetries observed at RHIC in $p+A$ collisions showed a surprisingly strong A dependence in inclusive forward neutron production. The observed asymmetry in $p+\mathrm{Al}$ collisions is much smaller, while the asymmetry in $p+\mathrm{Au}$ collisions is a factor of 3 larger in absolute value and of opposite sign. The interplay of different neutron production mechanisms is discussed as a possible explanation of the observed A dependence.

DOI: 10.1103/PhysRevLett.120.022001

Understanding forward particle production in high-energy hadron collisions is of great importance, because most of the energy goes in the forward direction, and therefore informs our understanding of overall particle production. This has particular importance in studies of ultrahigh-energy cosmic rays, where extraction of the cosmic ray distributions from air shower measurements depends on models of forward particle production in the interaction with nuclei in the air [1–3]. Mechanisms for forward particle production are not well understood, as perturbative quantum chromodynamics (pQCD) is not applicable at small momentum transfers and diffractive production mechanisms are not well modeled. To better understand production mechanisms, the measurement of the single-spin asymmetry A_N, describing the azimuthal asymmetry of particle production relative to the spin direction of the transversely polarized beam or target, provides crucial tests and deeper insight beyond just cross-section measurements. The spin degree of freedom has served as a strong discriminator between theoretical models. For example, the origin of the large asymmetries discovered in forward meson production in $p+p$ collisions from $\sqrt{s}=4.9$–19.4 GeV [4–11] and later confirmed at $\sqrt{s}=62.4$–500 GeV at the Relativistic Heavy Ion Collider (RHIC) [12–17] has been under intensive discussion for three decades and still remains an open question [18]. Despite substantial theoretical attempts to reproduce data in the pQCD regime using the conventional $2\to 2$ parton scattering processes, the latest multiplicity-dependent A_N measurements from RHIC [19] indicate that a significant contribution to the asymmetry may be of a diffractive nature.

Another important approach in forward particle production is to study the nuclear dependence in $p+A$ collisions. In the perturbative region, theoretical approaches based on color-glass-condensate models predicted that hadronic A_N should decrease with increasing A [20–24], while some approaches based on pQCD factorization predicted that A_N would stay approximately the same for all nuclear targets [25]. On the other hand, almost no theoretical or experimental studies are available in the nonperturbative region or diffractive scattering with polarized probes on nuclei, and interesting phenomena may be hidden in this unexplored region.

In the case of forward neutron production in $p+p$ collisions, production cross sections [26–28] were successfully explained in terms of one-pion exchange [29–33]. However, that model could not explain the sizable A_N in very forward (near zero degree) neutron production, discovered at RHIC in $p+p$ collisions at $\sqrt{s}=200$ GeV [28]. To reproduce the experimental asymmetry, an interference between the spin-flip π exchange and a non-spin-flip a_1-Reggeon exchange was necessary [33]. Kopeliovich, Potashnikova, and Schmidt considered nuclear absorption effects as a source for a possible A dependence of A_N and found only a small effect [34].

In this Letter, we report the first measurements of A_N for very forward neutron production in collisions between polarized protons and nuclei (Al and Au) at $\sqrt{s_{NN}}=200$ GeV recorded in 2015 with the PHENIX detector [35]. For $p+p$ collisions 18 RHIC stores were used and one store each for $p+\mathrm{Al}$ and $p+\mathrm{Au}$ measurements, with a typical store length of 8 h. The average beam polarization in $p+p$, $p+\mathrm{Al}$, and $p+\mathrm{Au}$ data samples was 0.515 ± 0.002, 0.59 ± 0.02, and 0.59 ± 0.04, respectively,

with an additional global uncertainty of 3% from the polarization normalization [36,37].

The experimental setup using a zero-degree calorimeter (ZDC) [38] and a position-sensitive shower-maximum detector (SMD) is similar to the one used for $p+p$ data [39]. The ZDC comprises three modules located in series at ± 18 m away from the collision point. The ZDC has an acceptance in the transverse plane of 10×10 cm^2, with a total of 5.1 nuclear interaction lengths (or 149 radiation lengths), and an energy resolution of ~25%–20% for 50–100 GeV neutrons. The SMD comprises x-y (horizontal-vertical) scintillator strip hodoscopes inserted between the first and second ZDC modules (approximately at the position of the maximum hadronic shower) and provides a position resolution of ~1 cm for 50–100 GeV neutrons. These detectors are located downstream of the RHIC DX beam splitting magnet, so that near beam-momentum charged particles from collisions are expected to be swept into the beam lines and out of the ZDC acceptance (see Fig. 1).

To accommodate asymmetric $p+A$ collisions of beams with different rigidity, the DX magnets were moved horizontally [40]. In this special setup for the present measurement, the proton beam was angled off axis by ~2 mrad relative to the nominal beam direction at the collision point, with a crossing angle with the Au (Al) beam of 2.0 (1.1) mrad. Correspondingly, the ZDC was moved by 3.6 cm (2 mrad) to keep zero-degree neutrons at the ZDC center (see Fig. 1).

The data were collected with triggers employing the ZDC and beam-beam counters (BBCs) [41]. Only the north ZDC detector, facing the incoming polarized proton beam, was used in this analysis. Two BBCs are located at ± 144 cm from the nominal collision point along the beam pipe and are designed to detect charged particles in the pseudorapidity range of $\pm(3.0$–$3.9)$ with full azimuthal coverage. The ZDC inclusive trigger required the energy deposited in the ZDC to be greater than 15 GeV. The ZDC ⊗ BBC-tag trigger in addition required at least one hit in each of the BBCs, and the ZDC ⊗ BBC-veto trigger required no hits in both BBCs. The latter two sets represent mutually exclusive but not complete subsets of the ZDC inclusive triggered data.

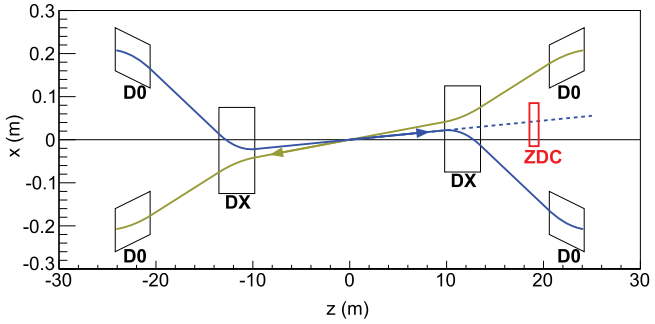

FIG. 1. ZDC location and beam orbits of a proton (blue) beam and a heavy-ion (yellow) beam in the special stores used for this analysis; the z axis shows the nominal beam direction, and the dashed line represents the zero-degree neutron trajectory. DX and D0 are the RHIC beam bending dipole magnets.

As described in detail in Ref. [39], event selection and neutron identification cuts include (i) a total ZDC energy cut of 40–120 GeV, (ii) at least two SMD strips fired (above threshold) in both x and y directions and a nonzero (above threshold) energy in the second ZDC module (to reject photons), and (iii) an acceptance cut of $0.5 < r < 4.0$ cm for the reconstructed radial distance r from the determined beam center (to reduce the impact of the position resolution and edge effects in the asymmetry measurements).

The raw asymmetry $[\epsilon_N(\phi)]$ is calculated using the square-root formula [39] for each azimuthal angle (ϕ) bin. The polarization normalized $A_N^{\rm fit}$ is then extracted from the fit to a sine function

$$\epsilon_N(\phi) = P A_N^{\rm fit} \sin(\phi - \phi_0), \tag{1}$$

where P is the proton beam polarization and ϕ_0 is the polarization direction in the transverse plane.

Figure 2 compares $\epsilon_N(\phi)/P$ results for ZDC inclusive samples from $p+p$, $p+$Al, and $p+$Au collisions and shows the nuclear dependence of $A_N^{\rm fit}$, including a sign change from negative in $p+p$ collisions to positive in $p+$Au collisions. The $A_N^{\rm fit}$ was measured separately in each PHENIX data-taking segment, typically 60 min long, and then the weighted average was calculated. The obtained $A_N^{\rm fit}$ is then corrected for backgrounds and detector responses. The main background contribution comes from protons, generated by elastic, diffractive, and hard processes.

Protons from elastic and diffractive reactions travel close to the beam line and are swept by the DX magnet to the right (toward negative x in Fig. 1). Only a small fraction of such protons scattered by large angles, larger than 4–5 mrad, fall in the ZDC acceptance. Because the cross section for these reactions falls sharply with the scattering angle, these protons contribute mainly on the right side of the ZDC. This contribution was evaluated from the particle position distribution as measured by the SMD and found to be 9% and 32% in the inclusive ZDC and ZDC ⊗ BBC-veto

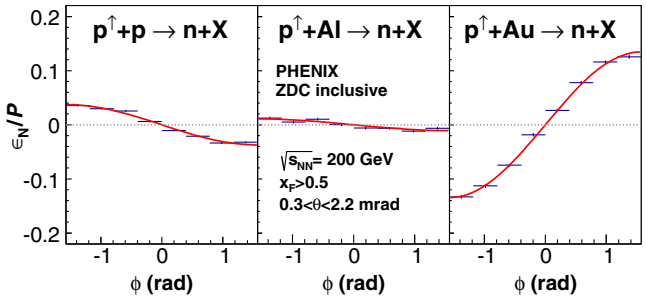

FIG. 2. $A_N^{\rm fit}$ fit of ZDC inclusive samples.

triggered samples, respectively, in $p+p$ collisions, $< 2\%$ in both samples in $p+A$ collisions, and negligible in ZDC $\otimes$ BBC-tag samples of both $p+p$ and $p+A$ collisions. The significant suppression of elastic and diffractive proton background relative to the neutron signal in $p+A$ collisions can be understood as due to the stronger magnetic fields in the DX magnets. Correspondingly, the minimum scattering angle for the elastic and diffractive proton backgrounds to reach the ZDC acceptance increases from 3.8 to 5 mrad, leading to a cross section reduction by an order of magnitude.

The contribution of the charged hadron background from hard scattering processes, distributed nearly uniformly over the ZDC acceptance, was estimated using PYTHIA6 [42] with a GEANT3 [43] detector simulation. However, from previous studies where a charge veto counter was installed in front of the ZDC to measure the charged hadron background, it was found that the simulation underestimates the proton background by a factor of ~ 2 [39]. Therefore, the hard scattering background contribution from the simulation was scaled by a factor of 2 with an uncertainty equal to the size of the increase. In $p+p$ collisions, this background fraction resulted in $6 \pm 3\%$, $3 \pm 1.5\%$, and $12 \pm 6\%$ in ZDC, ZDC $\otimes$ BBC-veto, and ZDC $\otimes$ BBC-tag triggered samples, respectively. In $p+A$ collisions, due to the increased neutron signal from electromagnetic (EM) processes (to be discussed later), the relative background contributions are expected to be smaller. Therefore, the measured asymmetries in $p+A$ collisions were not corrected for background, but one-sided systematic uncertainties (in the direction of the asymmetry magnitude increase) equal to the upper 1σ limit of the background fractions taken from the $p+p$ case, i.e., 9%, 4.5%, and 18%, were conservatively assigned in ZDC, ZDC $\otimes$ BBC-veto, and ZDC $\otimes$ BBC-tag triggered samples, respectively.

From the considerations above, only the $p+p$ asymmetries were corrected for backgrounds according to

$$A_N^S = \frac{A_N{}^{\text{fit}} - r_{\text{eff}} A_N^B}{1 - r_{\text{eff}}}, \tag{2}$$

where A_N^S and A_N^B stand for signal and background asymmetries, respectively, and r_{eff} is the "effective" background fraction in the reconstructed neutron sample. The parameter r_{eff} accounts for the dilution of the background effect in A_N^{fit} in the case when the background contributes preferably on one side of the detector (as from elastic or diffractive protons). This effect, which was studied in the simulation, comes from a specific way the left and right sides of detector acceptance are combined in the square-root formula for asymmetry calculation. The background asymmetry A_N^B was evaluated from the comparison of asymmetries with and without the charge veto cut from the 2008 data when the charge veto counter was available and then used in Eq. (2). The asymmetries A_N^B were found to be consistent with zero within statistical uncertainties for all triggers. After a background correction, A_N^S results for $p+p$ from 2008 and 2015 data were found to be consistent within statistical uncertainties. Asymmetries from 2015 data were used in the final results.

Besides charged hadrons, the other background sources are photons and K^0 mesons. From the PYTHIA6 simulation, their contribution after the analysis cuts was evaluated to be below 3% in all collision systems and triggers and was neglected in the asymmetry results.

The measured asymmetries are affected by detector resolutions and other detector systematic effects (e.g., edge effects), as well as by the uncertainty in the shape of the neutron production cross section vs p_T and x_F, the size of the asymmetry, and the assumption for the shape of $A_N(p_T)$ within the p_T range sampled in this analysis. These effects were studied in detail with a GEANT3 Monte Carlo simulation. The fully corrected transverse-single-spin asymmetry A_N was calculated as $A_N = A_N^S / C_\phi$, where the correction factor C_ϕ was calculated in the simulation as the ratio of the measured asymmetry to the average input asymmetry over the neutron sample collected with experimental cuts used in the analysis. The biggest variation in C_ϕ comes from the position resolution uncertainty and the assumption for $A_N(p_T)$. The position resolution in the simulation vs data was confirmed from the comparison of the shower shape and its fluctuations in SMD strips. The simulation was tuned to data by varying noise and thresholds in the SMD channels, as well as by introducing a cross talk effect, similar to Ref. [39]. An overall value of 3% was assigned to the C_ϕ uncertainty. For the shape of $A_N(p_T)$, it was modeled as $A_N(p_T) = \text{const}$ (as was assumed in Ref. [39]) and $A_N(p_T) \propto p_T$ (which is supported by theory in the p_T range relevant here [33]). The difference of 3% was included in the C_ϕ uncertainty. The final correction factor applied to the measured asymmetries is $C_\phi = 0.855 \pm 0.036$. Note that the C_ϕ value here is higher than the one in our previous publication [39] mainly due to two reasons: First, a more realistic $A_N(p_T) \propto p_T$ assumption was used in this analysis, and, second, the optimized SMD thresholds reduced the smearing effect.

In addition to the beam polarization, background, and smearing correction (C_ϕ) discussed above, the other sources of systematic uncertainties are the ZDC and SMD gain calibrations (including threshold variation) and location of the beam center on the ZDC plane. The latter is among the dominant uncertainties in this data, contributing 0.002–0.010 to the A_N uncertainty. It was estimated by calculating the asymmetry for varying assumptions of the beam axis projection on the ZDC plane, ± 1 cm in the horizontal and ± 0.5 cm in the vertical direction from the ZDC center, which reflect the uncertainty in ZDC alignment relative to the beam axis.

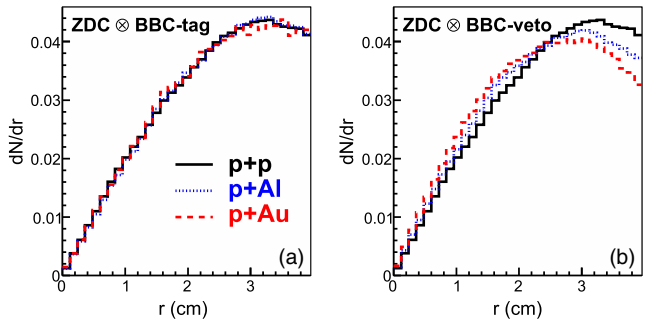

FIG. 3. The r distribution of the (a) ZDC ⊗ BBC-tag sample and (b) ZDC ⊗ BBC-veto sample for three collision systems.

The analyzed data correspond to the neutron sampled p_T in the range smaller than 0.25 GeV/c peaked at about 0.1 GeV/c, which is defined mainly by detector acceptance and which is affected by detector resolutions. Because of the varying contribution of different processes to neutron production, the sampled p_T distribution may vary in different collision systems and in different triggered data. Figure 3 shows the differences in the radial distributions, which is related to the neutron production cross section $d\sigma/dp_T$ by $p_T \propto r$ [39]. From a comparison with the simulation assuming different slope parameters b, in the parameterization $d\sigma/dp_T \sim e^{-b\cdot p_T}$, the data were found to be consistent with $b = 4$ $(\mathrm{GeV}/c)^{-1}$ for all collision systems in ZDC ⊗ BBC-tag triggered data and $b = 4$, 6, and 8 $(\mathrm{GeV}/c)^{-1}$ in $p+p$, $p+\mathrm{Al}$, and $p+\mathrm{Au}$ collisions, respectively, in a ZDC ⊗ BBC-veto triggered sample, with uncertainty $\sigma_b = 1$ $(\mathrm{GeV}/c)^{-1}$ reflecting its sensitivity to SMD gain calibration and thresholds. These variations lead to a difference in the average p_T sampled in different collision systems and triggers by as much as 10%. As can be also judged from Fig. 3, due to the small detector acceptance, the sampled p_T distribution shows a very modest dependence on the slope of the input p_T distribution, particularly at low p_T (or r), which is most responsible for the dilution of the measured asymmetry. As a consequence, the variation of the correction factor C_ϕ due to different slope parameters b discussed above was less than 1%.

Figure 4 and Table I summarize the results for A_N in forward neutron production in $p+p$, $p+\mathrm{Al}$, and $p+\mathrm{Au}$ collisions, for ZDC inclusive, ZDC ⊗ BBC-tag, and ZDC ⊗ BBC-veto samples. In addition to the 3% scale uncertainty from polarization normalization, common to all points, the other part of the polarization uncertainty is correlated for different triggers in a particular collision system. The presented asymmetries in $p+p$ collisions are consistent with our previous publication [39], albeit with larger systematic uncertainties in these data due to a larger background (unlike this measurement, the charged veto counter was used in Ref. [39] to suppress the background) and larger variations due to the uncertainty of the beam position on the ZDC plane.

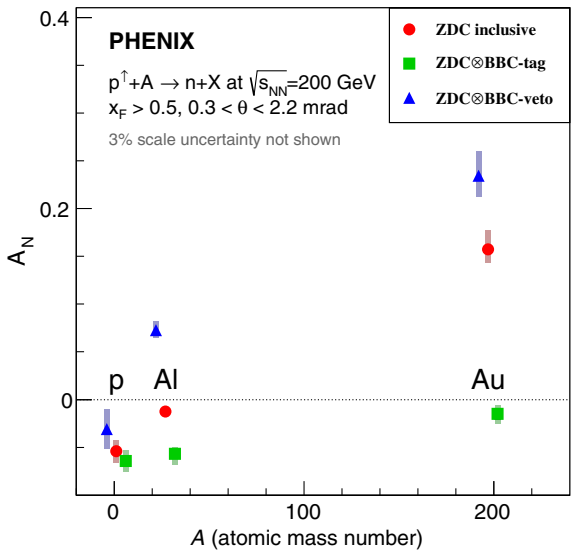

FIG. 4. Forward neutron A_N in $p+A$ collisions for $A = 1$ (p), 27 (Al), and 197 (Au), for ZDC inclusive, ZDC ⊗ BBC-tag, and ZDC ⊗ BBC-veto triggered samples; color bars are systematic uncertainties, and statistical uncertainties are smaller than the marker size; the 3% scale uncertainty (not shown) is from the polarization normalization uncertainty. Data points are shifted horizontally for better visibility.

From Fig. 4, the A dependence of A_N for inclusive neutrons is strong. Compared to the A_N of $p+p$ collisions, the observed asymmetry in $p+\mathrm{Al}$ collisions is much smaller, while the asymmetry in $p+\mathrm{Au}$ collisions is a factor of 3 larger in absolute value and of opposite sign. This behavior is unexpected, because the theoretical framework using π and a_1-Reggeon interference can predict only a moderate nuclear dependence, and there is no known mechanism to flip the sign of A_N within this framework [34].

The asymmetries requiring BBC hits are remarkably different. Once BBC hits are required (ZDC ⊗ BBC-tag), the drastic behavior of the inclusive A_N vanishes and its sign stays negative, approaching $A_N = 0$ at large A. In contrast, the strong A dependence is amplified once no hits in the BBC are required (ZDC ⊗ BBC-veto). While the BBCs cover a limited acceptance, the requirement (or veto) of hits in the BBC should place constraints on the activity near the detected neutron and thus the corresponding production mechanism.

One possibility to explain the present results is a contribution from EM interactions, which have been demonstrated to be important for reactions with small momentum transfer, e.g., in ultraperipheral heavy ion collision at RHIC [44–47] and Large Hadron Collider [48–51], including forward neutron production in $p+A$ collisions [52], and polarization observables in fixed target experiments [53,54]. Although it was ignored in the interpretation for the $p+p$ data [34], EM interactions become increasingly important for large atomic number (Z)

TABLE I. A_N for forward neutron production in $p+p$, $p+\mathrm{Al}$, and $p+\mathrm{Au}$ collisions, for ZDC inclusive, ZDC $\otimes$ BBC-tag, and ZDC $\otimes$ BBC-veto samples.

	$p+p$			$p+\mathrm{Al}$			$p+\mathrm{Au}$		
	Inclusive	BBC tag	BBC veto	Inclusive	BBC tag	BBC veto	Inclusive	BBC tag	BBC veto
A_N	-0.054	-0.064	-0.031	-0.013	-0.057	0.073	0.157	-0.015	0.234
Statistical uncertainty	±0.001	±0.002	±0.004	±0.002	±0.003	±0.003	±0.002	±0.005	±0.002
Systematic uncertainty:									
Background	±0.007	±0.009	±0.017	-0.001	-0.010	$+0.004$	$+0.015$	-0.003	$+0.012$
Smearing	±0.002	±0.003	±0.001	< 0.001	±0.002	±0.003	±0.007	< 0.001	±0.010
Beam position	±0.009	±0.006	±0.010	±0.004	±0.004	±0.006	±0.002	±0.004	±0.008
Polarization	< 0.001	< 0.001	< 0.001	< 0.001	±0.002	±0.003	±0.011	±0.001	±0.017
Calibration	±0.003	±0.001	±0.007	±0.001	±0.004	±0.004	±0.004	±0.009	±0.006
Total systematic	±0.012	±0.011	±0.021	$^{+0.004}_{-0.004}$	$^{+0.007}_{-0.012}$	$^{+0.009}_{-0.008}$	$^{+0.020}_{-0.014}$	$^{+0.009}_{-0.010}$	$^{+0.025}_{-0.022}$

nuclei, as the EM field of the nucleus is a rich source of virtual photons, increasing as Z^2. Forward neutrons in the final state can be produced through nonresonant photo-π^+ production and neutron decay channel from photonucleon excitation processes, such as the Δ resonance [55].

According to a Monte Carlo study [52], the neutron and its associated π^+ produced through this process are substantially boosted towards the proton beam direction, so that only a small fraction of pions would be detected by the BBC. Thus, a large fraction of EM processes are expected to be suppressed in the ZDC $\otimes$ BBC-tag events while enhanced in the ZDC $\otimes$ BBC-veto events. Here, it is noted that the importance of EM processes in $p+A$ collisions is also hinted at in the present data: The ratio between reconstructed neutrons in ZDC $\otimes$ BBC-veto and ZDC $\otimes$ BBC-tag samples increases from smaller than 0.5 in $p+p$ to $\sim$1 ($\sim$5) in $p+\mathrm{Al}$ ($p+\mathrm{Au}$) collisions. In addition, a faster drop of the neutron production cross section with p_T in $p+A$ collisions in ZDC $\otimes$ BBC-veto triggered data discussed in Fig. 3(b) is consistent with the increasing role of EM processes that have a softer p_T distribution than hadronic processes.

Similarly in the asymmetry measurements, contributions of different production mechanisms may be suppressed or enhanced by different event selection triggers. Hence, while the result for the ZDC $\otimes$ BBC-tag sample may be explained by the conventional pion and a_1-Reggeon interference mechanism [34], that for the ZDC $\otimes$ BBC-veto triggered sample could be explained by contributions from interference with EM amplitudes [55], which are expected to be enhanced in that data set. However, there could be other mechanisms, such as diffractive scattering, which is also expected to be enhanced by a ZDC $\otimes$ BBC-veto trigger. Therefore, further studies are needed to fully understand the present results.

In summary, we observe an unexpectedly strong A dependence in A_N of inclusive forward neutron production in polarized $p+A$ collisions at $\sqrt{s_{NN}} = 200$ GeV. Furthermore, a distinctly different behavior of A_N was observed in two oppositely trigger-enhanced data sets. These surprising behaviors could be explained by a contribution of EM interactions, which may be sizable for heavy nuclei. Further studies of the production mechanism including EM contributions and diffractive scattering would have an impact not only to hadron physics but also to cosmic-ray science, where measurements of high-energy cosmic rays depend on models of forward particle production in the interactions with nuclei in the air. Spin asymmetry measurements not only provide a unique discriminating power for the models of particle production but also will contribute to our understanding of the origin of the transverse spin asymmetries in hadronic collisions.

We thank the staff of the Collider-Accelerator and Physics Departments at Brookhaven National Laboratory, especially the CA-D staff for providing beams with a special tune for these measurements, and the staff of the other PHENIX participating institutions for their vital contributions. We also thank Boris Kopeliovich and Michal Křelina for providing us with theoretical calculations of the elastic proton cross sections and for useful discussions. We acknowledge support from the Office of Nuclear Physics in the Office of Science of the Department of Energy, the National Science Foundation, Abilene Christian University Research Council, Research Foundation of SUNY, and Dean of the College of Arts and Sciences, Vanderbilt University (USA), Ministry of Education, Culture, Sports, Science, and Technology and the Japan Society for the Promotion of Science (Japan), Conselho Nacional de Desenvolvimento Científico e Tecnológico and Fundação de Amparo à Pesquisa do Estado de São Paulo (Brazil), Natural Science Foundation of China (People's Republic of China), Croatian Science Foundation and Ministry of Science and Education (Croatia), Ministry of Education, Youth and Sports (Czech Republic), Centre National de la Recherche Scientifique, Commissariat à l'Énergie Atomique, and Institut National de Physique Nucléaire et de Physique des Particules (France), Bundesministerium für Bildung und Forschung, Deutscher Akademischer

Austausch Dienst, and Alexander von Humboldt Stiftung (Germany), J. Bolyai Research Scholarship, EFOP, the New National Excellence Program (ÚNKP), NKFIH, and OTKA (Hungary), Department of Atomic Energy and Department of Science and Technology (India), Israel Science Foundation (Israel), Basic Science Research Program through NRF of the Ministry of Education (Korea), Physics Department, Lahore University of Management Sciences (Pakistan), Ministry of Education and Science, Russian Academy of Sciences, Federal Agency of Atomic Energy (Russia), VR and Wallenberg Foundation (Sweden), the U.S. Civilian Research and Development Foundation for the Independent States of the Former Soviet Union, the Hungarian American Enterprise Scholarship Fund, the U.S.–Hungarian Fulbright Foundation, and the U.S.–Israel Binational Science Foundation.

[*]Deceased.
[†]PHENIX spokesperson.
akiba@rcf.rhic.bnl.gov

[1] D. d'Enterria, R. Engel, T. Pierog, S. Ostapchenko, and K. Werner, Constraints from the first LHC data on hadronic event generators for ultra-high energy cosmic-ray physics, Astropart. Phys. **35**, 98 (2011).
[2] K. H. Kampert and M. Unger, Measurements of the cosmic ray composition with air shower experiments, Astropart. Phys. **35**, 660 (2012).
[3] O. Adriani *et al.* (LHCf Collaboration), Measurements of longitudinal and transverse momentum distributions for neutral pions in the forward-rapidity region with the LHCf detector, Phys. Rev. D **94**, 032007 (2016).
[4] R. D. Klem, J. E. Bowers, H. W. Courant, H. Kagan, M. L. Marshak, E. A. Peterson, K. Ruddick, W. H. Dragoset, and J. B. Roberts, Measurement of Asymmetries of Inclusive Pion Production in Proton-Proton Interactions at 6 and 11.8 GeV/c, Phys. Rev. Lett. **36**, 929 (1976).
[5] W. H. Dragoset, J. B. Roberts, J. E. Bowers, H. W. Courant, H. Kagan, M. L. Marshak, E. A. Peterson, K. Ruddick, and R. D. Klem, Asymmetries in inclusive proton-nucleon scattering at 11.75 GeV/c, Phys. Rev. D **18**, 3939 (1978).
[6] J. Antille, L. Dick, L. Madansky, D. Perret-Gallix, M. Werlen, A. Gonidec, K. Kuroda, and P. Kyberd, Spin dependence of the inclusive reaction $p + p$(polarized) $\rightarrow \pi^0 + X$ at 24 GeV/c for high-p_T π^0 produced in the central region, Phys. Lett. **94B**, 523 (1980).
[7] S. Saroff *et al.*, Single-Spin Asymmetry in Inclusive Reactions $p^\uparrow + p \rightarrow \pi^+ + X$, $\pi^- + X$, and $p + X$ at 13.3 and 18.5 GeV/c, Phys. Rev. Lett. **64**, 995 (1990).
[8] C. E. Allgower *et al.*, Measurement of analyzing powers of π^+ and π^- produced on a hydrogen and a carbon target with a 22-GeV/c incident polarized proton beam, Phys. Rev. D **65**, 092008 (2002).
[9] D. L. Adams *et al.* (FNAL E704 Collaboration), Analyzing power in inclusive π^+ and π^- production at high $x(F)$ with a 200 GeV polarized-proton beam, Phys. Lett. B **264**, 462 (1991).
[10] D. L. Adams *et al.* (FNAL E581 and E704 Collaborations), First results for the two-spin parameter A_{LL} in π^0 production by 200 GeV polarized protons and antiprotons, Phys. Lett. B **261**, 197 (1991).
[11] D. L. Adams *et al.* (FNAL E704 Collaboration), Measurement of single spin asymmetry in η-meson production in $p^\uparrow p$ and $\bar{p}^\uparrow p$ interactions in the beam fragmentation region at 200 GeV/c, Nucl. Phys. **B510**, 3 (1998).
[12] I. Arsene *et al.* (BRAHMS Collaboration), Single-Transverse-Spin Asymmetries of Identified Charged Hadrons in Polarized pp Collisions at $\sqrt{s} = 62.4$ GeV, Phys. Rev. Lett. **101**, 042001 (2008).
[13] B. I. Abelev *et al.* (STAR Collaboration), Forward Neutral-Pion Transverse Single-Spin Asymmetries in $p + p$ Collisions at $\sqrt{s} = 200$ GeV, Phys. Rev. Lett. **101**, 222001 (2008).
[14] L. Adamczyk *et al.* (STAR Collaboration), Transverse single-spin asymmetry and cross section for π^0 and η mesons at large Feynman x in $p^\uparrow + p$ collisions at $\sqrt{s} = 200$ GeV, Phys. Rev. D **86**, 051101(R) (2012).
[15] A. Adare *et al.* (PHENIX Collaboration), Measurement of transverse-single-spin asymmetries for midrapidity and forward-rapidity production of hadrons in polarized $p + p$ collisions at $\sqrt{s} = 200$ and 62.4 GeV, Phys. Rev. D **90**, 012006 (2014).
[16] S. Heppelmann *et al.* (STAR Collaboration), Large p_T forward transverse single spin asymmetries of π^0 mesons at $\sqrt{s} = 200$ and 500 GeV from STAR, *Proc. Sci.*, DIS2013 (2013) 240.
[17] A. Adare *et al.* (PHENIX Collaboration), Cross section and transverse single-spin asymmetry of η mesons in $p^\uparrow + p$ collisions at $\sqrt{s} = 200$ GeV at forward rapidity, Phys. Rev. D **90**, 072008 (2014).
[18] E. C. Aschenauer *et al.*, The RHIC cold QCD plan for 2017 to 2023: A portal to the EIC, arXiv:1602.03922.
[19] M. M. Mondal (STAR Collaboration), Measurement of the transverse single-spin asymmetries for π^0 and jet-like events at forward rapidities at STAR in $p + p$ collisions at $\sqrt{s} = 500$ GeV, *Proc. Sci.*, DIS2014 (2014) 216.
[20] D. Boer, A. Dumitru, and A. Hayashigaki, Single transverse-spin asymmetries in forward pion production at high energy: Incorporating small-x effects in the target, Phys. Rev. D **74**, 074018 (2006).
[21] D. Boer and A. Dumitru, Polarized hyperons from pA scattering in the gluon saturation regime, Phys. Lett. B **556**, 33 (2003).
[22] D. Boer, A. Utermann, and E. Wessels, The saturation scale and its x-dependence from polarization studies, Phys. Lett. B **671**, 91 (2009).
[23] Z.-B. Kang and F. Yuan, Single spin asymmetry scaling in the forward rapidity region at RHIC, Phys. Rev. D **84**, 034019 (2011).
[24] Y. V. Kovchegov and M. D. Sievert, New mechanism for generating a single transverse spin asymmetry, Phys. Rev. D **86**, 034028 (2012).
[25] J.-W. Qiu, in *Proceedings of the RIKEN/RBRC Workshop: Forward Physics at RHIC, 2012, Upton, New York* (Brookhaven National Laboratory, Upton, 2012), Vol. 111, p. 741.

[26] J. Engler *et al.*, Measurement of inclusive neutron spectra at the ISR, Nucl. Phys. **B84**, 70 (1975).

[27] W. Flauger and F. Monnig, Measurement of inclusive zero-angle neutron spectra at the CERN ISR, Nucl. Phys. **B109**, 347 (1976).

[28] Y. Fukao *et al.*, Single transverse-spin asymmetry in very forward and very backward neutral particle production for polarized proton collisions at $\sqrt{s} = 200$ GeV, Phys. Lett. B **650**, 325 (2007).

[29] A. Capella, J. Tran Thanh Van, and J. Kaplan, Elastic scattering in perturbative Reggeon calculus, Nucl. Phys. **B97**, 493 (1975).

[30] B. Kopeliovich, B. Povh, and I. Potashnikova, Deep-inelastic electroproduction of neutrons in the proton fragmentation region, Z. Phys. C **73**, 125 (1996).

[31] N. N. Nikolaev, W. Schäfer, A. Szczurek, and J. Speth, Do the E866 Drell-Yan data change our picture of the chiral structure of the nucleon?, Phys. Rev. D **60**, 014004 (1999).

[32] A. B. Kaidalov, V. A. Khoze, A. D. Martin, and M. G. Ryskin, Leading neutron spectra, Eur. Phys. J. C **47**, 385 (2006).

[33] B. Z. Kopeliovich, I. K. Potashnikova, I. Schmidt, and J. Soffer, Single transverse spin asymmetry of forward neutrons, Phys. Rev. D **84**, 114012 (2011).

[34] B. Z. Kopeliovich, I. K. Potashnikova, and I. Schmidt, Leading Neutrons From Polarized Proton-Nucleus Collisions, AIP Conf. Proc. **1819**, 050002 (2017).

[35] K. Adcox *et al.* (PHENIX Collaboration), PHENIX detector overview, Nucl. Instrum. Methods Phys. Res., Sect. A **499**, 469 (2003).

[36] RHIC Polarimetry Group, RHIC/CAD Accelerator Physics Note No. 490, 2013.

[37] W. Schmidke (private communication).

[38] C. Adler, A. Denisov, E. Garcia, M. J. Murray, H. Strobele, and S. N. White, The RHIC zero degree calorimeters, Nucl. Instrum. Methods Phys. Res., Sect. A **470**, 488 (2001).

[39] A. Adare *et al.* (PHENIX Collaboration), Inclusive cross section and single transverse spin asymmetry for very forward neutron production in polarized $p + p$ collisions at $\sqrt{s} = 200$ GeV, Phys. Rev. D **88**, 032006 (2013).

[40] C. Liu *et al.*, in *Proceedings of the 7th International Particle Accelerator Conference (IPAC 2016): Busan, Korea, 2016* (CERN, Geneva, 2016), TUPMW038.

[41] M. Allen *et al.* (PHENIX Collaboration), PHENIX inner detectors, Nucl. Instrum. Methods Phys. Res., Sect. A **499**, 549 (2003).

[42] T. Sjöstrand, P. Edén, C. Friberg, L. Lönnblad, G. Miu, S. Mrenna, and E. Norrbin, High-energy-physics event generation with PYTHIA 6.1, Comput. Phys. Commun. **135**, 238 (2001).

[43] R. Brun *et al.*, Report No. CERN-W-5013, 1994.

[44] B. I. Abelev *et al.* (STAR Collaboration), ρ^0 photoproduction in ultraperipheral relativistic heavy ion collisions at $\sqrt{s_{NN}} = 200$ GeV, Phys. Rev. C **77**, 034910 (2008).

[45] S. Afanasiev *et al.* (PHENIX Collaboration), Photoproduction of J/ψ and of high mass e^+e^- in ultra-peripheral Au + Au collisions at $\sqrt{s_{NN}} = 200$ GeV, Phys. Lett. B **679**, 321 (2009).

[46] B. I. Abelev *et al.* (STAR Collaboration), Observation of $\pi^+\pi^-\pi^+\pi^-$ photoproduction in ultraperipheral heavy-ion collisions at $\sqrt{s_{NN}} = 200$ GeV at the STAR detector, Phys. Rev. C **81**, 044901 (2010).

[47] G. Agakishiev *et al.* (STAR Collaboration), ρ^0 photoproduction in AuAu collisions at $\sqrt{s_{NN}} = 62.4$ GeV measured with the STAR detector, Phys. Rev. C **85**, 014910 (2012).

[48] B. Abelev *et al.* (ALICE Collaboration), Coherent J/ψ photoproduction in ultra-peripheral Pb-Pb collisions at $\sqrt{s_{NN}} = 2.76$ TeV, Phys. Lett. B **718**, 1273 (2013).

[49] E. Abbas *et al.* (ALICE Collaboration), Charmonium and e^+e^- pair photoproduction at mid-rapidity in ultra-peripheral Pb-Pb collisions at $\sqrt{s_{NN}} = 2.76$ TeV, Eur. Phys. J. C **73**, 2617 (2013).

[50] B. B. Abelev *et al.* (ALICE Collaboration), Exclusive J/ψ Photoproduction off Protons in Ultraperipheral p-Pb Collisions at $\sqrt{s_{NN}} = 5.02$ TeV, Phys. Rev. Lett. **113**, 232504 (2014).

[51] J. Adam *et al.* (ALICE Collaboration), Coherent $\psi(2S)$ photo-production in ultra-peripheral Pb-Pb collisions at $\sqrt{s_{NN}} = 2.76$ TeV, Phys. Lett. B **751**, 358 (2015).

[52] G. Mitsuka, Forward hadron production in ultra-peripheral proton-heavy-ion collisions at the LHC and RHIC, Eur. Phys. J. C **75**, 614 (2015).

[53] I. G. Alekseev *et al.*, Measurements of single and double spin asymmetry in pp elastic scattering in the CNI region with a polarized atomic hydrogen gas jet target, Phys. Rev. D **79**, 094014 (2009).

[54] D. C. Carey *et al.*, Measurement of the Analyzing Power in the Primakoff Process with a High-energy Polarized Proton Beam, Phys. Rev. Lett. **64**, 357 (1990).

[55] G. Mitsuka, Recently measured large A_N for forward neutrons in $p\uparrow A$ collisions at $\sqrt{s_{NN}} = 200$ GeV explained through simulations of ultraperipheral collisions and hadronic interactions, Phys. Rev. C **95**, 044908 (2017).